FATIGUE PARAMETER BASED ON THE ASSESSMENT OF THE STRESS COMPONENTS ON ALL MATERIAL PLANES

C. LU, J. MELENDEZ, J. M. MARTÍNEZ–ESNAOLA

CEIT-IK4 and TECNUN (University of Navarra), Spain

A new fatigue parameter is proposed, which provides a new way of thinking to assess fatigue damage problems. The complete stress state at a certain material point, i.e., taking into account any material plane at that point, is included in this method. The influence of tension and compression state and also mean stress are also included. Some experiments with different materials and loading conditions are used to validate the capabilities of this method. The results show that the method provides good predictions for axial cyclic and/or torsion cyclic conditions with zero or non-zero mean stress, in-phase and out-of-phase, different shapes of the specimen, loading waveform and loading path.

Keywords: *fatigue parameter, mean stress effect, fatigue damage curve, complex loading, material planes.*

Introduction. Fatigue is one of the most common damage mechanisms in engineering components. The methods for evaluating fatigue damage can be divided into three main categories according to the mechanical magnitudes used in the definition of the different criteria, i.e. stress-based, strain-based and energy-based methods. As a general rule, stress-based methods are used in high-cyclic fatigue, strain-based methods are used in low-cyclic fatigue and can also be used in high-cyclic fatigue and energy-based methods can be used in both high- and low-cyclic fatigue because they contain contributions of both stress and strain magnitudes. Basically, in the stress/strain-based methods, maximum normal or shear stress/strain is used in tension fatigue or torsion fatigue, and then some simple modifications like amplitude, mean value, separation between elastic/plastic components are used. The stress invariant like J_2, or hydrostatic pressure σ_H, or some equivalent stress/strain like Mises, Tresca, etc. are also used to predict fatigue damage.

More complex formulations assume that fatigue damage should take into account the stress or strain components (typically, normal and shear components) that can be active on different planes at a given material point. For instance in [1] a fatigue parameter (FP) given by $\Delta\gamma_{max}/2 + S\Delta\varepsilon_n$, where $\Delta\gamma_{max}$ is the range of maximum shear strain, $\Delta\varepsilon_n$ is the range of normal strain on the plane of maximum range of shear strain and S is a material constant, is proposed. It is therefore assumed that both shear and normal strain can affect fatigue damage, shear strain is the predominant factor in crack formation and at the first stages of crack development, and normal strain is dominant during macrocrack propagation. The authors of [2] have modified the Kandil method as $\Delta\gamma_{max}/2 + (1 - \sigma_n/2\sigma_y)\Delta\varepsilon_n$, where σ_n is normal stress on the plane of maximum range of shear strain and σ_y is yield limit. In this modification the influence of normal stress can be taken into consideration. The influence of normal loading with the help of the maximum normal stress σ_n^{max}, in the form $0.5\Delta\gamma_{max}[1 + k\sigma_n^{max}/\sigma_y]$, where k is a material constant, is considered in [3]. In this method it is assumed that the fatigue damage is mainly affected by the maximum shear strain range; the maximum normal stress is only used as a correcting term to revise the influence of maximum shear strain range.

Corresponding author: C. LU, e-mail: clu@ceit.es

The energy-based methods assume that the fatigue damage is controlled by the energy dissipation in the cyclic loading, represented by the hysteretic loop in the stress-strain plot. Fatigue parameter $\sigma_1^{max}\Delta\varepsilon_1/2$, where σ_1^{max} is the maximum principal stress and $\Delta\varepsilon_1$, is the range of principal strain, is presented in [4]. Note that it represents the tractive part of a sort of hysteretic loop in a fully reversed cycle. In this approach normal energy is used to calculate fatigue damage, which is accurate when tensile failure of the material is predominant. Fatigue parameter in the form $0.25\Delta\gamma_{12}\Delta\sigma_{12}[1/(1 - \sigma_{12}^{max}/\sigma_f') + 1/(1 - \sigma_{22}^{max}/\sigma_f')]$, where $\Delta\gamma_{12}$ is the range of shear strain; $\Delta\sigma_{12}$ is the range of shear stress; $\Delta\sigma_{12}^{max}$ is the maximum shear stress; $\Delta\sigma_{22}^{max}$ is the maximum normal stress; τ_f' and σ_f' are shear and normal fatigue strength limit, is defined in [5]. In this method it is assumed that the shear energy provides the main contribution to fatigue damage and, at the same time, both maximum shear and normal stresses have some influence on fatigue damage. Authors of [6] combine two above methods and suggest the parameter $\Delta\varepsilon_1\Delta\sigma_1 + k\Delta\gamma_1\Delta\tau_1$, where $\Delta\sigma_1$, $\Delta\tau_1$ are the range of normal and shear stress, respectively; $\Delta\gamma_1$, $\Delta\varepsilon_1$ are the range of shear and normal strain, respectively and k is a material constant. It is assumed in this method that both shear and normal energy can affect fatigue damage and the relative contribution of shear and normal energy is quantified by the parameter k. Further modifications are proposed in [7] as $\Delta\sigma_n\Delta\varepsilon_n/\sigma_f'\varepsilon_f' + (1 + \sigma_n^m/\sigma_f')(\Delta\tau_{max}\Delta(0.5\gamma_{max}))/\tau_f'\gamma_f'$, where σ_n^m is the mean normal stress; τ_f' and σ_f' are shear and normal fatigue strength coefficients; ε_f' and γ_f' are normal and shear fatigue ductility coefficients. In this method the influence of mean normal stress σ_n^m is taken into consideration.

A new proposed fatigue parameter. The different approaches to assessing fatigue damage reviewed in the previous section indicate that the stress/strain-based methods are essentially based on normal/shear, stress/strain, and some modification such as those due to the range, (maximum and mean) or a combination of some of them (the methods based on energy magnitudes can be an example).

The presented approach is based on generalizing the idea that normal and shear components of the stress and strain are different on different planes at a certain material point further to the simple combination of maximum stress or strain values. The definition of the new fatigue parameter is described below. The well-known Mohr's circle representation of the stress (or strain) state will be used to illustrate the main ideas of the proposed method.

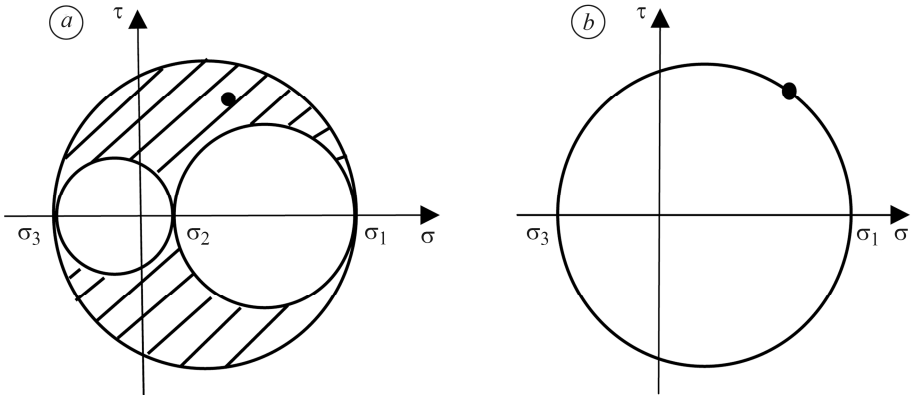

Fig. 1. Mohr's stress circle: *a* – 3D stress; *b* – plane stress.

Figure 1 presents the Mohr's stress circle for the 3D stress state (Fig. 1*a*) and the plane stress state (Fig. 1*b*). The black point in the figure represents the normal and shear stress components on a certain material plane. In the methods sketched in the

previous section only some stress/strain components at a certain point (or maybe two) are used to calculate fatigue damage. Although the stress (or strain) state at a material point is fully described by the Mohr's representation, fatigue damage is, in general, dependent on the normal and shear stress (or strain) components on a given plane. Therefore we need a method to quantify the amount of damage on each plane and find a weighting procedure to define the equivalent fatigue damage parameter at that point. The possible combinations of normal/shear stress are represented by the shadowed region in the 3D Mohr's stress circle in Fig. 1*a*, and by the whole circumference for plane stress conditions (Fig. 1*b*). The new fatigue parameter is defined as follows:

$$\mathrm{FP} = \frac{\sum \Delta D \cdot \Delta P}{P}, \tag{1}$$

where ΔD is fatigue damage on a certain material plane at a certain material point which is a function of σ and τ, and ΔP is the contribution of each material plane to the total set of possible planes, the summation is extended to all material planes, P is the summation of all ΔP. In this way all stress/strain components at a certain material point can be taken into consideration. We do not need to choose some specific components as the representative components to calculate the fatigue damage. This overcomes the shortcoming of the methods above. The mathematical form of Eq. (1) for the 3D and 2D stress (or strain) states can be written as Eq. (2), where $\Delta S/S$ is the area section in the 3D Mohr's stress circle and $\Delta L/L$ is the arc length section in the plane of the Mohr's stress circle:

$$\mathrm{FP} = \frac{\sum \Delta D \cdot \Delta S}{S}; \qquad \mathrm{FP} = \frac{\sum \Delta D \cdot \Delta L}{L}. \tag{2}$$

As the stress components on a certain material plane can be reduced to a normal component and a shear component, we define the fatigue damage ΔD as:

$$\Delta D = \mu(A|\sigma| + B|\tau|), \tag{3}$$

where A and B are coefficients describing the influence of normal and shear stress components, respectively, on fatigue damage. In order to make sure that the influence of both normal and shear stress is positive, A and B should be greater than zero. In this paper it is assumed that the influence of normal and shear stresses is the same, $A=B$. Here the absolute value of τ is used because of the up-down symmetry of τ in the Mohr's circle, otherwise the mean influence of τ would be zero as a result of the averaging procedure. In order to make sure that the fatigue damage is positive, the absolute value of σ is used; μ is used to represent the different influence of tension and compression loading and is defined as follows:

$$\mu = \begin{matrix} +1 & \sigma_m \geq 0, \\ -1 \cdot \omega & \sigma_m < 0, \end{matrix} \tag{4}$$

in which σ_m is the mean stress and ω is the coefficient to describe the influence of compression. The value of ω is assumed to be 1 in this paper, which means that tension and compression have the same influence. In the multiaxial loading conditions FP can be calculated as

$$\mathrm{FP} = \mathrm{FP}_{\max} - \mathrm{FP}_{\min}, \tag{5}$$

where $\mathrm{FP}_{\max}$ and $\mathrm{FP}_{\min}$ are the maximum and minimum value of the FP in a cycle. According to this new method we can consider three cases for calculating the fatigue parameter in both the 3D stress state and plane stress state (see Fig. 2) depending on the sign of the principal stresses. The first case corresponds to the situation where the minimum principal stress is greater than or equal to zero, as in Figs. 2*a* and *d*; the

second case is when the maximum principal stress is less than or equal to zero, as in Figs. 2*b* and *e*; and the third case is when the maximum principal stress is greater than zero and the minimum principal stress is less than zero as in Figs. 2*c* and *f*.

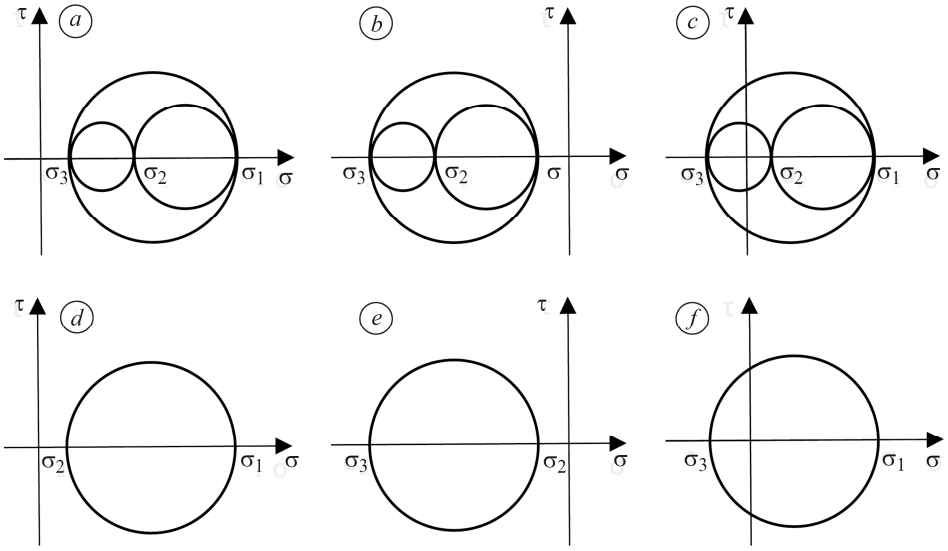

Fig. 2. Different stress states for the 3D and plane stress state:
a–c – 3 cases of 3D; *d–f* – 3 cases of plane.

Sensitivity analysis. Here we consider some simple cases to show the influence of the change of principal stresses on the FP according to this method. We use Figs. 2*d*, *e* as examples to show the influence of the principal stress. In this discussion we assume that only one principal stress is changing to have a comparison of the different influence of the change of each of the different principal stresses. For the case in Fig. 2*d* we have the rates of the FP variation as follows (the details of the calculations are given in the appendix)

$$\frac{\partial FP}{\partial \sigma_1} = \frac{A}{2} + \frac{B}{\pi}; \qquad \frac{\partial FP}{\partial \sigma_2} = \frac{A}{2} - \frac{B}{\pi}. \tag{6}$$

Similarly, for the case in Fig. 2*e* we get

$$\frac{\partial FP}{\partial \sigma_2} = -\frac{A}{2} + \frac{B}{\pi}; \qquad \frac{\partial FP}{\partial \sigma_3} = -\frac{A}{2} - \frac{B}{\pi}. \tag{7}$$

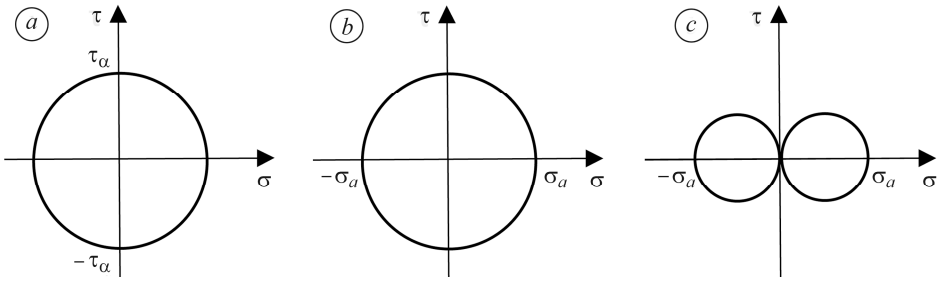

Fig. 3. Some cases with the same stress amplitude: *a* – fully reversed torsion;
b – fully reversed biaxial tension-compression; *c* – fully reversed axial.

We can notice that for the case in Fig. 2*d*, where *A* and *B* are greater than zero, the value of the FP increases with the increase of σ_1, and the influence of σ_1 on the FP is bigger than that of σ_2. The value of σ_2 only has a positive influence on the FP when the

value of A/B is bigger than $2/\pi$. For the case in Fig. 2*e* the influence of σ_2 is bigger than that of σ_3 and σ_3 always has a negative influence on the FP. Also, when the value of A/B is smaller than $2/\pi$, σ_2 has a positive influence on the FP. For other cases the influence of the principal stresses variation is more complex and each case should be considered separately.

Some other special cases, such as fully reversed torsion, fully reversed biaxial tension-compression and fully reversed axial loading conditions with the same stress amplitude are depicted in Fig. 3. It can be seen that according to the new parameter proposed in this paper, the fatigue damage in fully reversed torsion and biaxial opposite tension-compression conditions with the same stress amplitude is the same, while it is different from the fatigue damage in fully reversed axial loading conditions.

Results and experimental validation. In order to check the capabilities of this new proposed fatigue parameter, some experimental results with different materials subjected to different loading conditions are used. Figs. 4*a–c* represent experimental measurements in fatigue under axial and torsion loading conditions. Tests shown in Fig. 4*a* were conducted in a fully reversed axial and fully reversed torsion loading conditions with zero mean stress. Tests in Fig. 4*b* correspond to axial and torsion loading conditions with zero or non-zero mean stress. Tests in Fig. 4*c* were conducted in axial and torsion loading conditions with zero mean stress and with different specimen shapes. It can be noticed that for the single axial or single torsion loading conditions with different materials, different shapes of the specimen and zero or non-zero mean stress, the prediction with the new proposed fatigue parameter is pretty good.

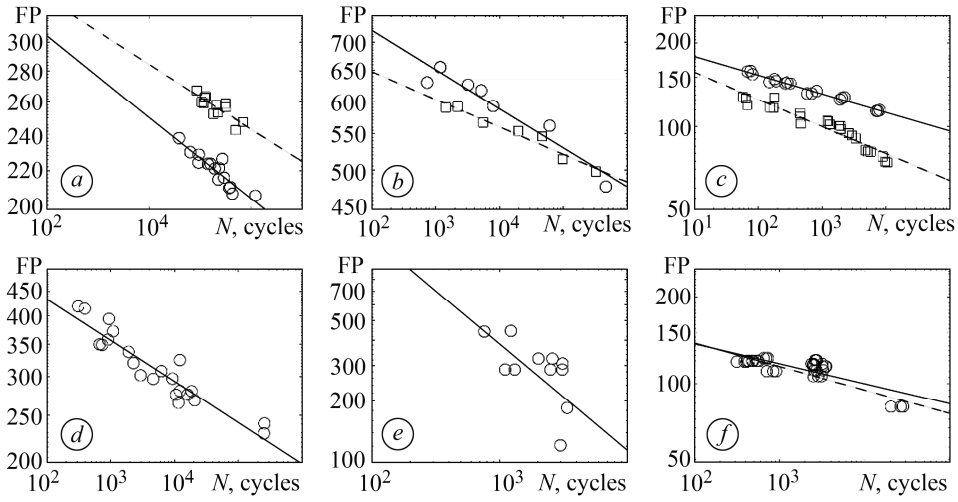

Fig. 4. Dependences of the FP on number of cycles (N) for different materials: *a* – S355 J2 [8], *b* – SNCM630 [9], *c* – AW-2007 [10] (○ – reversed axial (experiment); ⎯⎯ – reversed axial (prediction); □ – reversed torsion (experiment); - - - - – reversed torsion (prediction)); *d* – Haynes 188 [11] (○ – in/out of phase axial+torsion (experiment); ⎯⎯ – in/out of phase axial+torsion (prediction)); *e* – 42CrMo [12] (○ – complex loading (experiment); ⎯⎯ – complex loading (prediction)); *f* – AW-2007 [10] (○ – complex loading (experiment), ⎯⎯ – complex loading (fitting), - - - - – complex loading (prediction)).

There is an experimental evidence of differences between the axial and torsion fatigue damage curves [8, 10], as a clear indication that fatigue damage depends on the loading conditions. Most experimental results are for axial and torsional loading. In order to predict the fatigue damage in the more complex loading conditions, such as axial-torsion loading, in-phase and out-of-phase loading and even random loading, which contain various combinations of normal and shear stresses, it is assumed here

that fatigue damage curve in complex loading conditions, $F(\mathrm{FP}_c, N_c)$, can be predicted by an axial fatigue damage curve $Q(\mathrm{FP}_a, N_a)$ and a shear fatigue damage curve $W(\mathrm{FP}_t, N_t)$:

$$F(\mathrm{FP}_c, N_c) = f(\xi Q, \zeta W). \tag{8}$$

The parameters ξ and ζ represent the influence of the axial and torsion loading conditions. These can be thought of as the relative contributions to the fatigue damage curve in the complex loading condition, axial loading conditions and torsion conditions, respectively. For example, if $\xi/\zeta = 1$, the fatigue damage curve in complex loading conditions is the angle bisector of fatigue damage curves in axial and torsion loading conditions.

The results of the test shown in Fig. 4*d* were conducted in an in-phase and out-of-phase axial-torsion loading conditions with different values of mean stress, different phase difference and different shape of the loading waveform. Because both axial and torsional loadings are included in these loading conditions we can use these data to get the fatigue damage curve for the complex loading conditions directly. It can be seen that the proposed method provides a good agreement. Tests in Fig. 4*e* correspond to a more complex loading condition with different shapes of the load path. It can be seen that the results are also good, within a factor of two, accepted as reasonable in fatigue experiments.

Tests in Fig. 4*f* correspond to the same material as those in Fig. 4*c*, but the loading conditions are more complex, containing different load paths. Firstly, we use Eq. (8) to predict fatigue damage curve in the complex loading conditions with the help of axial and torsion fatigue damage curve but without using data generated in the complex loading conditions. Then the experimental fatigue results in the complex loading conditions are compared with the predicted fatigue damage curve. The complex loading conditions have different loading paths but all load paths satisfy $\varepsilon_{max}/\gamma_{max}=3^{0.5}$, so it is assumed here that the influence coefficient $\xi/\zeta = 3^{0.5}$. This means that the fatigue curve in this particular complex loading condition is closer to the fatigue damage curve in the axial loading condition. It can be seen that the predicted fatigue damage curve is almost the same as that based on direct fitting for the experimental data.

CONCLUSIONS

In this paper a new fatigue parameter is proposed which suggests a new way of thinking to tackle the fatigue damage problems. The difference between this new method and other existing methods is that there is no need to choose some certain stress, strain or energy components on a certain material plane as representative parameters to calculate fatigue damage. The stress components on every material plane at a certain material point are averaged and included in this method which can show all features of the stress state at a certain material point. In this new method the difference between tension and compression state and the influence of the mean stress are accounted for.

Some experiments with different materials and different loading conditions are used to validate the capabilities of the proposed method both for data representation and for life prediction. The loading conditions considered in the validation include reversed axial, reversed torsion, axial cycling with non-zero mean stress, torsion cycling with non-zero mean stress, different types of the specimen, different shapes of loading waveform, in-phase and out-of-phase loading and different loading paths. The results show that this new method provides good correlations and predictions for all these materials and loading conditions.

Appendix

For the case in Fig. 2*d*, the FP is calculated as: $\mathrm{FP} = \dfrac{\oint (A|\sigma| + B|\tau|) \cdot ds}{L}$.

The integral is performed in terms of the angle describing the Mohr's circle, between 0 and π, according to the symmetry of τ in the Mohr's circle, as explained in the text:

$$\mathrm{FP} = \frac{2\int_0^{\pi}\left[A\left(\frac{\sigma_1-\sigma_2}{2}\cos\theta+\frac{\sigma_1+\sigma_2}{2}\right)+B\frac{\sigma_1-\sigma_2}{2}\sin\theta\right]\frac{\sigma_1-\sigma_2}{2}d\theta}{\pi(\sigma_1-\sigma_2)}.$$

And finally, $\frac{\partial \mathrm{FP}}{\partial\sigma_1}=\frac{A}{2}+\frac{B}{\pi}$; $\frac{\partial \mathrm{FP}}{\partial\sigma_2}=\frac{A}{2}-\frac{B}{\pi}$.

РЕЗЮМЕ. Запропоновано новий метод оцінювання втомних пошкоджень, який враховує напружений стан у певній точці матеріалу. Взято до уваги вплив розтягу і стиску, а також середнього значення напруження. Випробувано різні матеріалами та досліджено різні умови навантаження. Виявлено, що метод придатний для прогнозування умов виникнення осьових циклічного напруження чи закруту з нульовим чи ненульовим середнім значенням, що збігаються чи не збігаються за фазою, для різних геометрій зразків, форми циклу та траєкторії навантаження.

РЕЗЮМЕ. Предложен новый метод оценки усталостных повреждений, который учитывает напряженное состояние в некоторой точке материала. Принято во внимание влияние растяжения и сжатия, а также среднего значения напряжения. Испытаны различные материалы и исследованы разные условия нагружения. Выявлено, что метод пригоден для прогнозирования условий возникновения осевых циклических напряжения или кручения с нулевым или ненулевым средним значением, которые совпадают или не совпадают по фазе, для различных геометрий образцов, формы цикла и траектории нагружения.

1. *Kandil F. A., Brown M. W., and Miller K. J.* Biaxial low-cycle fatigue failure of 316 stainless steel at elevated temperatures // Proc. Int. Conf. "Mechanical behaviour and nuclear applications of stainless steel at elevated temperatures". – 1982. – **14**, № 22. – P. 203–209.
2. *Wang Y. Y. and Yao W. X.* A multiaxial fatigue criterion for various metallic materials under proportional and non-proportional loading // Int. J. Fatig. – 2006. – **28**, № 4. – P. 401–408.
3. *Fatemi A. and Socie D. F.* A critical plane approach to multiaxial fatigue damage including out-of-phase loading // Fatig. & Fract. Eng. Mat. & Struct. – 1988. – **11**, № 3. – P. 149–165.
4. *Smith K. N., Topper T. H., and Watson P.* A stress-strain function for the fatigue of metals (stress-strain function for metal fatigue including mean stress effect) // J. Mat. – 1970. – **5**, № 4. – P. 767–778.
5. *Glinka G., Wang G., and Plumtree A.* Mean stress effects in multiaxial fatigue // Fatig. & Fract. of Eng. Mat. & Struct. – 1995. – **18**, № 7–8. – P. 755–764.
6. *Itoh T., Sakane M., and Ohsuga K.* Multiaxial low cycle fatigue life under non-proportional loading // Int. J. Pressure Vessels and Piping. – 2013. – **110**. – P. 50–56.
7. *Varvani-Farahani A.* A new energy-critical plane parameter for fatigue life assessment of various metallic materials subjected to in-phase and out-of-phase multiaxial fatigue loading conditions // Int. J. Fatig. – 2000. – **22**, № 4. – P. 295–305.
8. *High* and low cycle fatigue life estimation of welding steel under constant amplitude loading: Analysis of different multiaxial damage models and in-phase and out-of-phase loading effects / C. Gómez, M. Canales, S. Calvo, et al. // Int. J. Fatig. – 2011. – **33**, № 4. – P. 578–587.
9. *Han C., Chen X., and Kim K. S.* Evaluation of multiaxial fatigue criteria under irregular loading // Int. J. Fatig. – 2002. – **24**, № 9. – P. 913–922.
10. *Szusta J. and Seweryn A.* Fatigue damage accumulation modelling in the range of complex low-cycle loadings –The strain approach and its experimental verification on the basis of EN AW-2007 aluminum alloy // Int. J. Fatig. – 2011. – **33**, № 2. – P. 255–264.
11. *Kalluri S. and Bonacuse P. J.* In-phase and out-of-phase axial-torsional fatigue behavior of haynes 188 superalloy at 760 C // Adv. in Multiaxial Fatig. ASTM Int. – 1993.
12. *Kang G., Liu Y., and Ding J.* Multiaxial ratcheting–fatigue interactions of annealed and tempered 42CrMo steels: experimental observations // Int. J. Fatig. – 2008. – **30**, № 12. – P. 2104–2118.

Received 23.03.2017